Short Circuit Behavior of Dual Three-phase Permanent Magnet Synchronous Motors with Different Mutual Inductance in Electric Propulsion Application

Yinghui Yang and Georg Möhlenkamp
BRANDENBURGISCHE TECHNISCHE UNIVERSITÄT
Platz der Deutschen Einheit 1
Cottbus, Germany
Tel.: +49 (0) 355 69 5571
Fax: +49 (0) 355 69 4019
E-Mail: Yinghui.Yang@b-tu.de
URL: https://www.b-tu.de/fg-lea

Acknowledgements

The authors would like to acknowledge the helpful advice provided by Rolls-Royce Deutschland Ltd & Co KG. This research is funded by ILB - ProFIT Red Eagle under Project: P32055003

Keywords

« Permanent magnet motor », « Multiphase drive », « Mutual inductance », « Short circuit », « Fault tolerance », « Electric Propulsion »

Abstract

The dual three-phase permanent magnet synchronous motors (DTP-PMSMs) are suitable in aircraft electric propulsion unit (EPU) application because of their good reliability and fault-tolerant capability. However, this fault-tolerant capability can get weakened or even eliminated in short circuit fault due to the influence of flux coupling between the two isolated three-phase sub-systems. In this paper, a mathematical model of DTP-PMSMs with different mutual inductance between the two sub-systems is developed and analyzed. Based on the model, different short circuit protection methods are discussed and compared. Finally, a simulation of an EPU consisting of a DTP-PMSM, and a simplified constant speed propeller (CSP), is implemented to verify the short circuit behaviors.

Introduction

A typical DTP-PMSM consists of two isolated three-phase sub-systems. Compared with conventional three-phase PMSM, DTP-PMSM is more reliable due to the redundant winding configuration. For example, when there is one-point open circuit fault occurring in one sub-system, the another healthy sub-system is still able to delivery half of the nominal torque[1]. However, this benefit may not work in short circuit condition. The widely used protection method in PMSM short circuit fault is active short circuit (ASC), which creates a symmetrical short circuit in the unhealthy three-phase system with a symmetrical short circuit current flow through all three phases[2]. With two sub-systems in DTP-PMSM, there are two possible ASC options if a short circuit fault occurs internally in one sub-system. One option is only applying ASC on the unhealthy sub-system and let the healthy sub-system keep operating , which is known as active-shorted mode (ASM-ASC). Another option is applying ASC on both sub-systems, known as shorted-shorted mode (SSM-ASC)[3][4]. On the other hand, two isolated sub-systems can have flux coupling through the shared flux path, known as the mutual inductance, between the two sub-systems. With this mutual inductance, the current in one sub-system can induce EMF in another sub-system, making the two sub-systems no longer independent. Therefore, it is important to study the influence of this mutual inductance on machine operation, especially under short circuit condition, to optimize the selection of the short circuit protection method.

Machine model

In different stator winding arrangements of DTP-PMSM, the mutual inductance between two sub-systems is different. Depending on the significance of the mutual inductance, the DTP-PMSMs can be classified into two types, the one with high mutual inductance between two sub-systems (HM-DTP-PMSM) and the one with low mutual inductance between two sub-systems (LM-DTP-PMSM). Typical stator winding arrangements of both types are shown in Fig. 1 (a) and (b), where ABC represents windings of one sub-system (abc-sub-system) and XYZ represents windings of the another sub-system (xyz-sub-system). A 30-degree electrical angle shift between the two sub-systems is applied for both types[5].

Designing the stator winding arrangement is a comprehensive topic. For example, if the number of cores per slot is the same in both types of DTP-PMSM in Fig. 1, the flux linkage, and the d- and q-axis inductances will not be the same in those two types, finally resulting in different motor parameters and operation conditions, making it difficult to compare[6]. Since the influence of mutual inductance between two sub-systems is the main research object in this paper, the following assumptions are made:

1. different motors are designed in such a way that the main operation parameters are the same, as Table I shows, and only mutual inductance between two sub-systems is variable.
2. the d-axis and q-axis are identical for both sub-systems, and the inductance fluctuation is ignored with round rotor.

Table I: Parameters of DTP-PMSM

Parameter	Symbol	Value
Nominal power	$P_{(n)}$	50kW
Nominal torque	$T_{e(n)}$	205Nm
Nominal speed	$N_{m(n)}$	2320rpm
Nominal d-axis current	$i_{d(n)}$	0A
Nominal q-axis current	$i_{q(n)}$	200A
PM flux linkage	Ψ_{PM}	0.04366Wb
Phase resistance	R_s	0.01Ohm
Total d-axis inductance	L_d	300uH
Total q-axis inductance	L_q	300uH
Number of pole-pairs	P_p	8

To study the influence of mutual inductance, it is simple to use the dual dq-coordinate frame in building the mathematical model of DTP-PMSM, since the mutual inductance between the two sub-systems is a direct variable in dual dq-transformation[7]. The voltage equations are shown in (1) to (4), where number 1 and 2 represent two sub-systems, u_d and u_q are d-axis and q-axis voltages, i_d and i_q are d-axis and q-axis currents, Ψ_d and Ψ_q are d-axis and q-axis flux linkages, and ω_e is electrical rotational speed.

$$u_{d1} = R_s i_{d1} + \frac{d\Psi_{d1}}{dt} - \omega_e \Psi_{q1} \quad (1)$$

$$u_{q1} = R_s i_{q1} + \frac{d\Psi_{q1}}{dt} + \omega_e \Psi_{d1} \quad (2)$$

$$u_{d2} = R_s i_{d2} + \frac{d\Psi_{d2}}{dt} - \omega_e \Psi_{q2} \quad (3)$$

$$u_{q2} = R_s i_{q2} + \frac{d\Psi_{q2}}{dt} + \omega_e \Psi_{d2} \quad (4)$$

The flux linkage equations of the DTP-PMSM in dual dq-coordinate frame is shown in (5) to (8), where L_{dd} and L_{qq} are d-axis and q-axis self-inductances, M_{dd} and M_{qq} are the d-axis and q-axis mutual inductances.

$$\Psi_{d1} = i_{d1}L_{dd} + i_{d2}M_{dd} + \Psi_{PM} \quad (5)$$
$$\Psi_{q1} = i_{q1}L_{qq} + i_{q2}M_{qq} \quad (6)$$
$$\Psi_{d2} = i_{d2}L_{dd} + i_{d1}M_{dd} + \Psi_{PM} \quad (7)$$
$$\Psi_{q2} = i_{q2}L_{qq} + i_{q1}M_{qq} \quad (8)$$

The torque produced by the DTP-PMSM can be calculated as (9) to (11).

$$T_{e1} = 1.5 \cdot P_p\left(\Psi_{d1}i_{q1} - \Psi_{q1}i_{d1}\right) \quad (9)$$
$$T_{e2} = 1.5 \cdot P_p\left(\Psi_{d2}i_{q2} - \Psi_{q2}i_{d2}\right) \quad (10)$$
$$T_e = T_{e1} + T_{e2} \quad (11)$$

The total d- and q-axis inductances, which are assumed to be designed as constant value in different stator winding arrangements, can be calculated as (12) and (13)

$$L_d = L_{dd} + M_{dd} \quad (12)$$
$$L_q = L_{qq} + M_{qq} \quad (13)$$

A new variable k is employed in the mathematical model, to express the ratio of the mutual inductance to the self-inductance of both the d- and q-axis, as shown in (14) and (15)

$$M_{dd} = k \cdot L_{dd} \quad (14)$$
$$M_{qq} = k \cdot L_{qq} \quad (15)$$

Theoretically, the maximum value of k can reach up to 1, meaning the mutual inductance between two sub-systems is equal to the self-inductance. Therefore, the range of k is from 0 to 1. Specifically, in different stator winding arrangements, winding function (WF) approach can be used to calculate the self-inductances and the mutual inductances of all dual three-phase stator windings[8]. This inductance matrix can be transferred into dual dq-coordinate frame and then the k value can be calculated. The winding function of both DTP-PMSMs are demonstrated in Fig. 1 (c) and (d). The calculated $k_{HM-DTP-PMSM}$ is 0.86, and the calculated $k_{LM-DTP-PMSM}$ is 0.

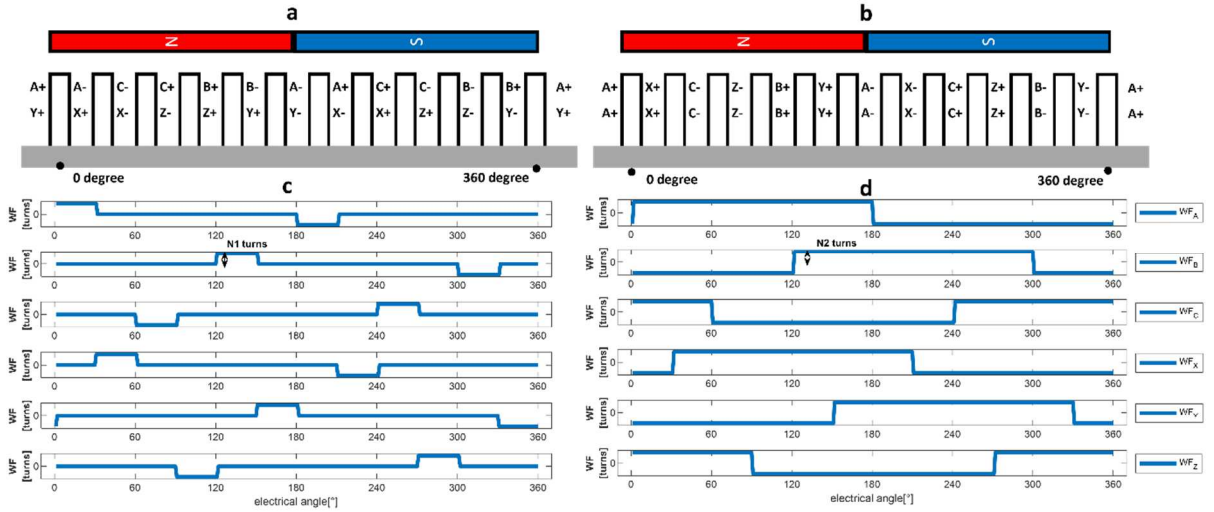

Fig.1: Two typical DTP-PMSM stator arrangements with its winding function (WF). (a) stator arrangement of LM-DTP-PMSM. (b) stator arrangement of HM-DTP-PMSM. (c) winding function of LM-DTP-PMSM. (d) winding function of HM-DTP-PMSM

Active short circuit

In SSM-ASC, the d- and q-axis voltages in both sub-systems become zero. According to machine model, the d- and q-axis currents of both shorted sub-systems can be calculated as (16) and (17).

$$i_{d_{SSM-ASC}} = -\frac{\omega_e^2 \Psi_{PM} L_q}{\omega_e^2 L_d L_q + R_s^2} \tag{16}$$

$$i_{q_{SSM-ASC}} = -\frac{\omega_e \Psi_{PM} R_s}{\omega_e^2 L_d L_q + R_s^2} \tag{17}$$

In ASM-ASC, the d- and q-axis voltages in unhealthy sub-system become zero. In the healthy sub-system, the d- and q-axis voltages are still controllable. Field oriented control (FOC) is widely used in electrical machine controls. Usually, the inner loop of the FOC is current regulator, which controls the d- and q-axis currents, respectively. In DTP-PMSM, two independent current regulators in the FOC inner loop, one for each sub-system, are used. Therefore, we can assume the d- and q-axis currents in the healthy sub-system can be still controlled as the set values. According to machine model, the d- and q-axis currents in the shorted sub-system can be calculated as (18) and (19), where i_d^* and i_q^* represent the controlled values of the d- and q-axis currents in the healthy sub-system.

$$i_{d_{ASM-ASC}} = -\frac{\omega_e^2 \Psi_{PM} L_q (k+1) - \omega_e L_q R_s i_q^* k(k+1) + \omega_e^2 L_d L_q i_d^* k}{\omega_e^2 L_d L_q + (k+1)^2 R_s^2} \tag{18}$$

$$i_{q_{ASM-ASC}} = -\frac{\omega_e \Psi_{PM} R_s (k+1)^2 + \omega_e L_d R_s i_d^* k(k+1) + \omega_e^2 L_d L_q i_q^* k}{\omega_e^2 L_d L_q + (k+1)^2 R_s^2} \tag{19}$$

According to (9) to (11) and (16) to (19), the steady state operation status of the DTP-PMSM versus motor speed after ASC can be plotted as shown in Fig. 2, where the i_d^* and i_q^* in ASM-ASC are assumed to be controlled as nominal values. It can be seen from the figure that the k value has a significant influence on motor operation if motor does ASM-ASC, while no influence if motor does SSM-ASC. When the motor speed is high, the influence of stator resistance is neglectable compared with the influence from inductance. Therefore, in a wide range of motor speed, the motor current and motor torque keep almost constant, in both ASM-ASC and SSM-ASC.

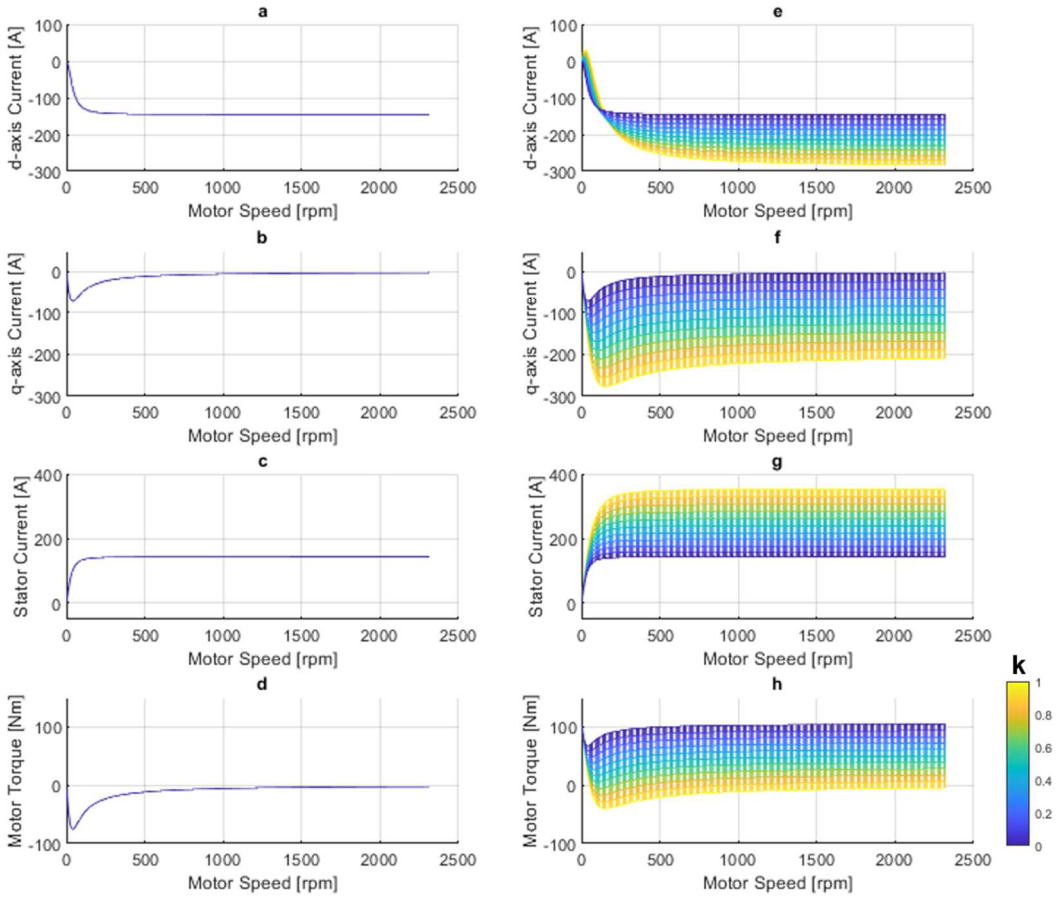

Fig. 2: Theoretical analysis of steady state operation status versus motor speed of unhealthy sub-system in DTP-PMSM during SSM-ASC (the four sub-graphs at left column) and ASM-ASC (the four sub-graphs at right column, color bar represents different k). (a) and (e) d-axis current. (b) and (f) q-axis current. (c) and (g) magnitude of stator current. (d) and (h) motor torque.

When motor speed is high, the d-axis current in the shorted sub-system in both SSM-ASC and ASM-ASC is demagnetizing current. In SSM-ASC, this value is around -145.5A for one sub-system, totally -291A for both sub-systems. In ASM-ASC, as k increases, this value increases from -145.5A to -284A. Therefore, in terms of demagnetizing effect, ASM-ASC is better for LM-DTP-PMSM.

The higher stator current usually causes higher loss in the stator windings. The symmetrical short circuit current after SSM-ASC is not necessary to be lower than motor nominal stator current, sometimes it can be higher, depending on the motor design. In the motor used in this paper , the nominal magnitude of the stator current is 200A. In SSM-ASC, the magnitude of the stator current in both sub-systems is 145.5A that is lower than the nominal value. In ASM-ASC, as k increases, the magnitude of the stator current in the shorted sub-system increases from 145.5A up to 353A. Therefore, in terms of magnitude of the state current, ASM-ASC is not a good option for HM-DTP-PMSM.

One important purpose for doing ASM-ASC is to gain some remaining torque through the healthy sub-system when short circuit fault occurs in DTP-PMSM. However, as k increases, the remaining motor torque decreases from half of the nominal torque to almost 0 Newtonmeter, even with d- and q-axis currents controlled to be as nominal values in the healthy sub-system. Due to this deceasing remaining torque, the HM-DTP-PMSM has a weaker fault tolerance capacity in terms of short circuit fault, compared to LM-DTP-PMSM.

Therefore, it can be concluded from the above discussion that ASM-ASC is more suitable for LM-DTP-PMSM, and SSM-ASC is more suitable for HM-DTP-PMSM.

Simulation

To investigate the short circuit behaviors in EPU, a simulation model is built in MATLAB/Simulink. The simulation model consists of two main parts, one DTP-PMSM connected at one end of the shaft, and one torque source with rotational speed feedbacked PI controller to simulate the simplified CSP behavior, connected at another end of the shaft. The DTP-PMSM has the same parameters as in the Table I. Two ideal switch based three-phase voltage source inverters (B6-VSIs) are used to drive the DTP-PMSM with a switching frequency 10kHz. The DTP-PMSM is controlled to operate with nominal d- and q-axis current by FOC. The PI controller in the simplified CSP is tuned to have a long reaction time that is in approximate range of 5 seconds. Shaft inertia is assumed to be 3 kilogram-meter squared. Friction is ignored. The short circuit fault occurs in abc-sub-system at 0.5 Second. Both LM-DTP-PMSM and HM-DTP-PMSM shown in Fig. 1 are simulated.

The simulation results of ASM-ASC in LM- and HM-DTP-PMSM are shown in Fig. 3. It can be observed that the DTP-PMSMs with different k values show significantly different behaviors after ASM-ASC. Since it is expected that the motor can still deliver torque in ASM-ASC, the speed controller in CSP will keep working to maintain the shaft speed to be as the nominal value. The process of ASM-ASC can be mainly divided into two parts based on shaft speed. The first part is shaft speed transient, in which the shaft speed drops and the CSP tries to recover the speed. The second part is short circuit steady state, in which the shaft speed maintains again back as nominal by CSP. In both parts of the process, the abc-sub-system in DTP-PMSM does ASC and the xyz-sub-system maintains its d- and q-axis current as nominal values by its FOC current regulator. In LM-DTP-PMSM, the healthy xyz-sub-system can still deliver approximately half of the nominal torque. The magnitude of the stator current in the shorted abc-sub-system is around 145A, and the stator current in xyz-sub-system maintains nominal value. One problem in this scenario is the d-axis current in abc-sub-system that does demagnetizing of the PM with a value of -145A. In HM-DTP-PMSM, the performance becomes even worse. The short circuit transient peak current reaches above 500A, which is more than twice higher than nominal current. With the impact of xyz-sub-system, the peak value of the steady state short circuit current in the unhealthy abc-sub-system increases to 400A. The d-axis current in the unhealthy abc-sub-system becomes -250A which can cause worse demagnetizing problem on the PM. The q-axis current of around -180A in the unhealthy abc-sub-system, together with the q-axis current in the healthy xyz-sub-system that is controlled to be as nominal value, results in a remaining torque close to 0 Newtonmeter.

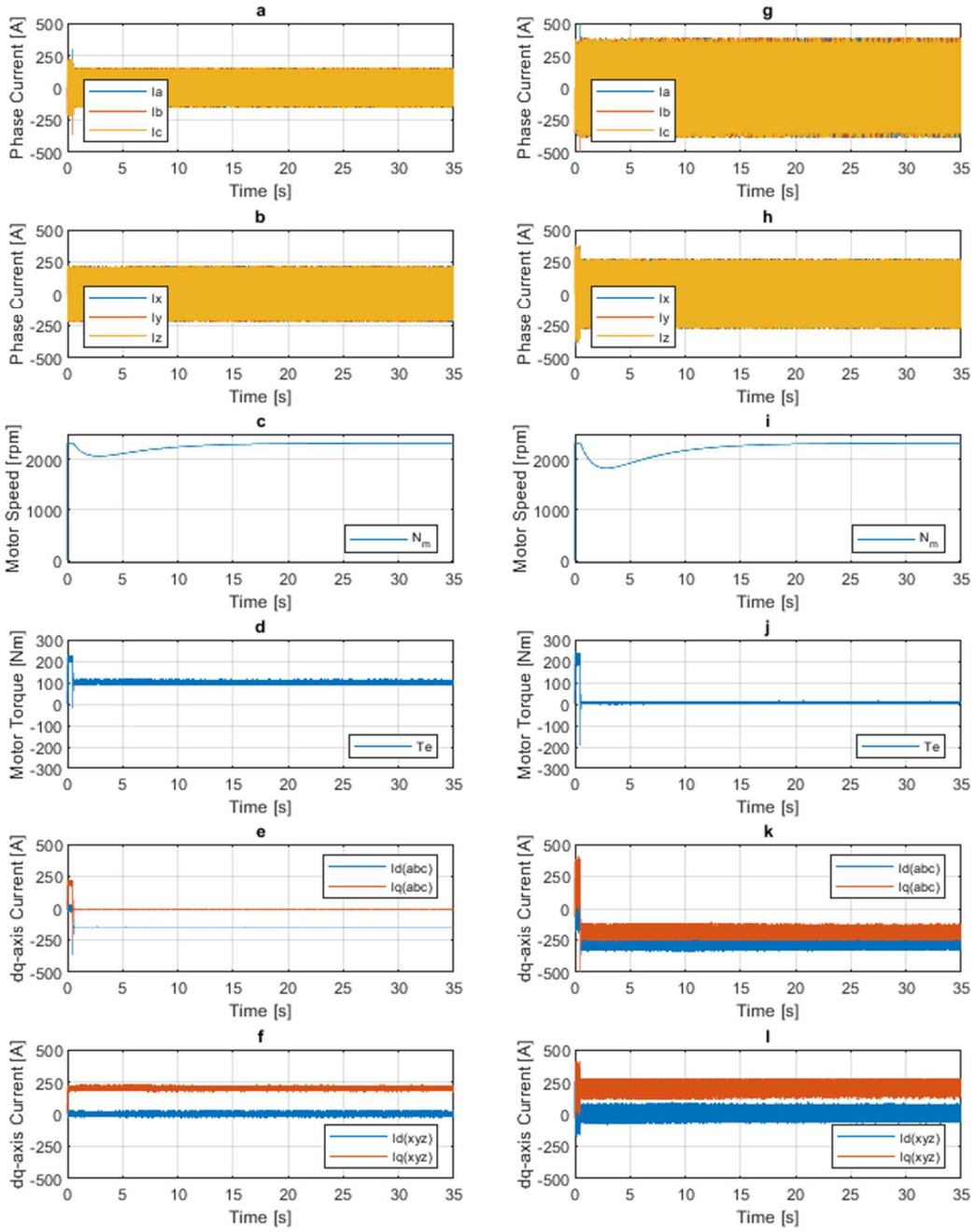

Fig. 3: Simulation results of ASM-ASC in LM-DTP-PMSM (the six sub-graphs at left column) and in HM-DTP-PMSM (the six sub-graphs at right column). (a) and (g) abc-sub-system phase current. (b) and (h) xyz-sub-system phase current. (c) and (i) motor speed. (d) and (j) motor torque. (e) and (k) dq-axis current of abc-sub-system. (f) and (l) dq-axis current of xyz-sub-system.

The simulation results of SSM-ASC in LM- and HM-DTP-PMSM are shown in Fig. 4. Since it is expected that the motor will lose all torque in SSM-ASC, simplified feathering process of the CSP is simulated after 17.5 Second. The process of SSM-ASC can be mainly divided into three parts. The first and the second parts are similar like in ASM-ASC, where the shaft speed will first drop and then get recovered. The third part is feathering, in which the shaft speed will decelerate to a very low value. It can be observed that the motors with different k values behave similarly after SSM-ASC in all three parts. Before the end of feathering, the magnitude of stator current remains around 145A, and the motor torque remains at a small negative value. When the shaft speed is low enough, the motor braking torque will increase up to -73 Newtonmeter that can even help to brake the shaft faster.

After the peak braking torque, as the shaft speed further decreases, the braking torque, as well the stator current, decreases simultaneously. In the entire process, there is no over current or over torque problem. One problem that can be observed is the demagnetizing current in d-axis, which remains around -145A in both sub-systems until the end of feathering.

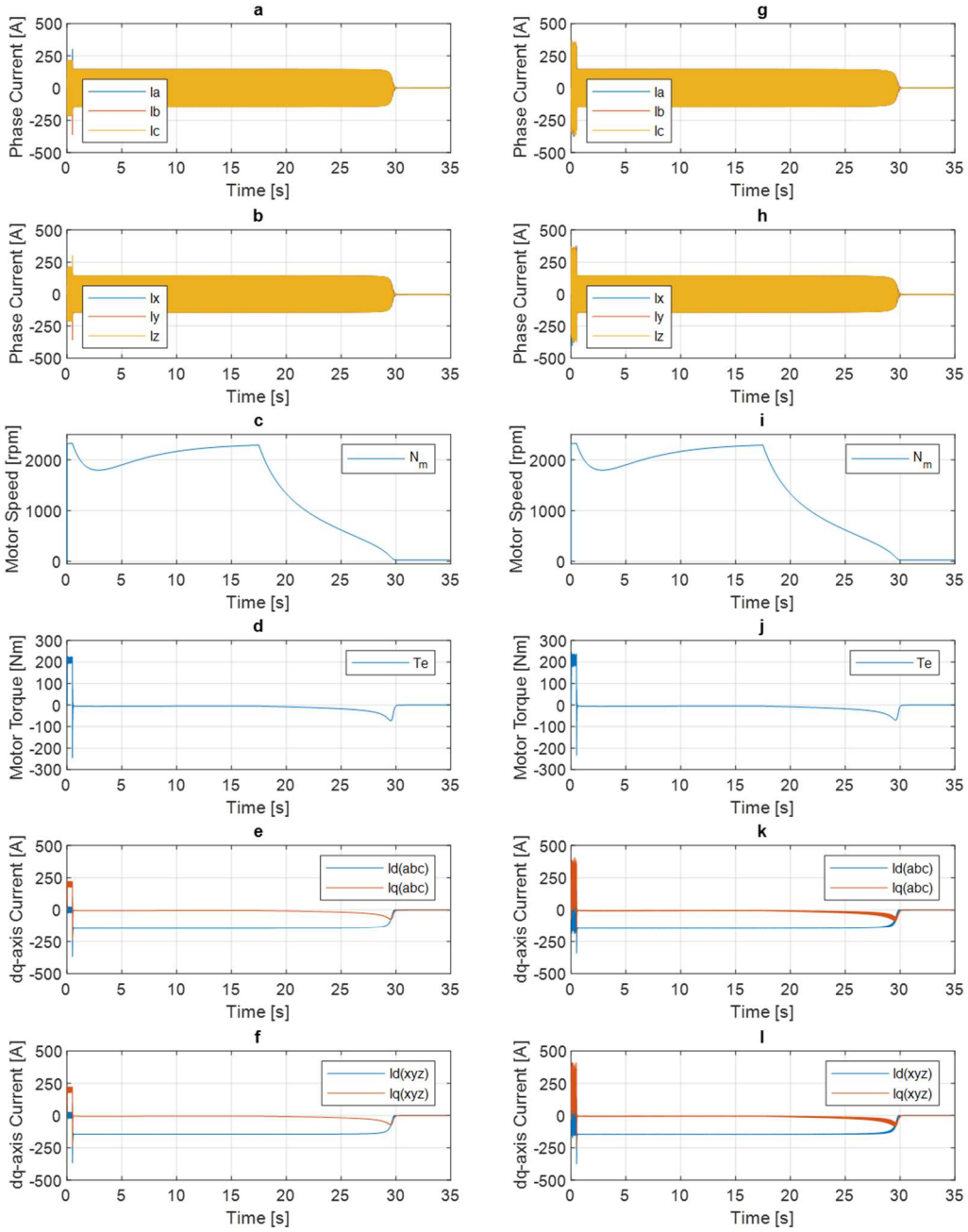

Fig. 4: Simulation results of SSM-ASC in LM-DTP-PMSM (the six sub-graphs at left column) and in HM-DTP-PMSM (the six sub-graphs at right column). (a) and (g) abc-sub-system phase current. (b) and (h) xyz-sub-system phase current. (c) and (i) motor speed. (d) and (j) motor torque. (e) and (k) dq-axis current of abc-sub-system. (f) and (l) dq-axis current of xyz-sub-system.

The simulation results of phase current and motor torque zoomed in ASC transient are shown in Fig. 5. It can be observed that both LM-DTP-PMSM and HM-DTP-PMSM can operate at similar points if the main electrical parameters are designed to be the same, even with significantly different mutual inductance between two sub-systems. With higher mutual inductance between two sub-systems, the stator current ripple becomes higher because one sub-system current can induce EMF on the another sub-system and finally creates higher ripple in the stator current. The over current during transient in HM-DTP-PMSM with ASM-ASC is the highest one in all scenarios, which is almost twice higher than

others. The torque oscillation is similar in HM-DTP-PMSM with ASM-ASC ,and LM- and HM-DTP-PMSM with SSM-ASC, which is almost twice higher than in LM-DTP-PMSM with ASM-ASC. The overall transient time is around 30 milliseconds.

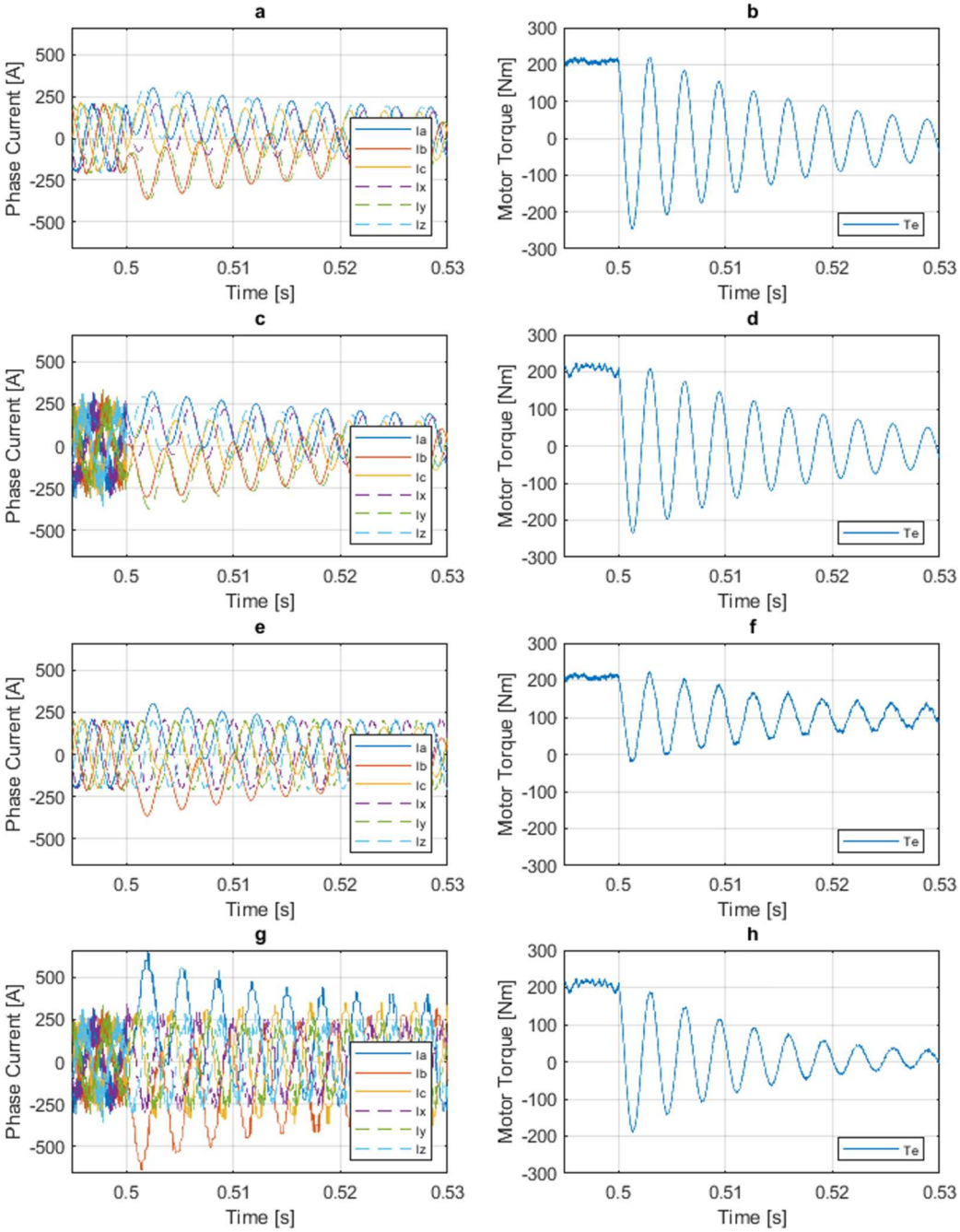

Fig. 5: Simulation results of phase current and motor torque during ASC transient. The four sub-graphs at left column are phase current. The four sub-graphs at right column are motor torque. (a) and (b) from LM-DTP-PMSM with SSM-ASC. (c) and (d) from HM-DTP-PMSM with SSM-ASC. (e) and (f) from LM-DTP-PMSM with ASM-ASC. (g) and (h) from HM-DTP-PMSM with ASM-ASC.

Conclusion

This paper focuses on the short circuit behaviors of DTP-PMSM. The influence of mutual inductance between two sub-systems is studied and analyzed under two different ASC methods, the ASM-ASC and the SSM-ASC. A mathematical model of DTP-PMSM is developed in this paper for the study. One innovative point of this mathematical model is to use a simple variable k to express the ratio of the

mutual inductance to the self-inductance. The variable k represents the significance of the mutual inductance in total d- and q- axis inductance directly. Based on this mathematical model, analytical expressions of the steady state dq-axis current and the motor torque of both ASC methods are derived respectively. By changing k values, comparative analysis has been completed on demagnetizing effect, magnitude of the steady state ASC stator current, and remaining motor torque for both ASC methods. To validate the theoretical result, a simulation model of an EPU is built in MATLAB/Simulink. For each ASC method, both HM-DTP-PMSM and LM-DTP-PMSM are simulated. With dynamic DTP-PMSM and CSP models, both transient and steady state behaviors of EPU after ASC can be observed. The steady state ASC behaviors of DTP-PMSM from the simulation can verify the mathematical model. According to both theoretical analysis and the simulation result, if the mutual inductance between two sub-systems is low, the ASM-ASC performs better compared with SSM-ASC due to the sufficient remaining motor torque. Inversely, the SSM-ASC performs better if the mutual inductance between two sub-systems is high, due to less steady state stator current.

References

[1] D. Michieletto, N. Bianchi and M. Brunetti, "Dual Three-phase Motor Fault Tolerance for Modern Transport," 2021 International Aegean Conference on Electrical Machines and Power Electronics (ACEMP) & 2021 International Conference on Optimization of Electrical and Electronic Equipment (OPTIM), 2021, pp. 405-412, doi: 10.1109/OPTIM-ACEMP50812.2021.9590040.

[2] B. A. Welchko, T. M. Jahns, W. L. Soong and J. M. Nagashima, "IPM synchronous machine drive response to symmetrical and asymmetrical short circuit faults," in IEEE Transactions on Energy Conversion, vol. 18, no. 2, pp. 291-298, June 2003, doi: 10.1109/TEC.2003.811746.

[3] P. Giangrande, V. Madonna, S. Nuzzo, C. Gerada and M. Galea, "Braking Torque Compensation Strategy and Thermal Behavior of a Dual Three-Phase Winding PMSM During Short-Circuit Fault," 2019 IEEE International Electric Machines & Drives Conference (IEMDC), 2019, pp. 2245-2250, doi: 10.1109/IEMDC.2019.8785164.

[4] M. Kozovsky, P. Blaha.: Double three-phase PMSM structures for fail operational control, IFAC-PapersOnLine, Volume 52, Issue 27,2019, Pages 1-6, ISSN 2405-8963,

[5] M. Barcaro, N. Bianchi and F. Magnussen, "Faulty Operations of a PM Fractional-Slot Machine With a Dual Three-Phase Winding," in IEEE Transactions on Industrial Electronics, vol. 58, no. 9, pp. 3825-3832, Sept. 2011, doi: 10.1109/TIE.2010.2087300.

[6] A. M. EL-Refaie and T. M. Jahns, "Optimal flux weakening in surface PM machines using fractional-slot concentrated windings," in IEEE Transactions on Industry Applications, vol. 41, no. 3, pp. 790-800, May-June 2005, doi: 10.1109/TIA.2005.847312.1

[7] Y. Hu, Z. Q. Zhu and M. Odavic, "Comparison of Two-Individual Current Control and Vector Space Decomposition Control for Dual Three-Phase PMSM," in IEEE Transactions on Industry Applications, vol. 53, no. 5, pp. 4483-4492, Sept.-Oct. 2017, doi: 10.1109/TIA.2017.2703682.

[8] Z. Liang, D. Liang and S. Jia, "Inductance Calculation for the Symmetrical Non-Salient Dual Three-Phase PMSM Based on Winding Function Approach," 2018 21st International Conference on Electrical Machines and Systems (ICEMS), 2018, pp. 269-274, doi: 10.23919/ICEMS.2018.8549109.